Research on Engineering Structures & Materials
www.jresm.org
Research Group

Thermal and crack behavior of reinforced high-performance concrete edge-restrained wall

Yasameen N. K. Albresha, Hussam K. Risan

Online Publication Date: 30 December 2025

URL: http://www.jresm.org/archive/resm2026-1265ic1015rs.html
DOI: http://dx.doi.org/10.17515/resm2026-1265ic1015rs

Journal Abbreviation: *Res. Eng. Struct. Mater.*

To cite this article
Albresha Y N K, Risan H K. Thermal and crack behavior of reinforced high-performance concrete edge-restrained wall. *Res. Eng. Struct. Mater.*, 2026; 12(2): 1067-1085

Research on Engineering Structures & Materials
www.jresm.org
Research Group

Research Article

Thermal and crack behavior of reinforced high-performance concrete edge-restrained wall

Yasameen N. K. Albresha [*,a], Hussam K. Risan [b]

Department of Civil Engineering, Al-Nahrain University, Baghdad, Iraq

Article Info

Article History:

Received 15 Oct 2025

Accepted 26 Dec 2025

Keywords:

Early-age cracking;
High-performance concrete(HPC);
Edge-restrained wall;
Hydration of cement;
Durability.

Abstract

This study experimentally investigates the early-age behavior of edge-restrained concrete walls constructed with normal-strength (NSC) and high-performance concrete (HPC) under realistic outdoor conditions. The research quantifies temperature variations, strain development, and cracking potential, focusing on the influence of length-to-height (L/H) ratios and reinforcement details. Key findings reveal that while HPC exhibited over twice the tensile strength of NSC, micro-cracking at the aggregate-mortar interface was prevalent in all walls, precluding macro-crack formation during the observation period. Increasing the L/H ratio led to a significant increase in peak shrinkage strains, with HPC walls showing up to 9.1% higher values in longer walls. These results underscore the critical importance of considering the interplay between concrete mix design (particularly tensile strength), structural geometry (L/H ratio), and environmental factors to optimize the durability and minimize early-age cracking risks in restrained concrete structures.

1. Introduction

Early-age cracking is a major problem in reinforced concrete supporting structures, especially those that are used in hydraulic provisions. This effect is produced by suppressed post-cast alterations in volume. The volumetric changes are triggered by a combination of factors, such as heat production of shrinkage, creep, cement hydration, and seasonal variations of environmental conditions. Concrete members are in practice seldom free, either being restrained internally by reinforcement or restrained externally by the support of neighboring structural members. This restriction of volumetric variations causes cracks formation in reinforced concrete structures. The management and reduction of cracking to manageable levels, though not to zero, is still attainable despite its impossibility to do away with it completely.

A fair amount of work has been put into the characterisation of early-age cracking behaviour in restrained concrete members, with special attention paid to edge-restrained designs. The research done early [1-4] was on the mechanism of shrinkage and thermal cracking in reinforced mortar walls, which examined the occurrence of the first and subsequent cracks in the base restrained walls. The studies produced good information on the effect of the length-height ratio (L/H) on the formation of cracks, where it was noted that cracks are more common in the walls with an L/H ratio that is more than about 2.5. Mushchil et al. [5] studied end and edge-restrained mortar using the walls as test material and found that cracking was more prevalent than previously because the end restraints were present. Al-Tameemi et al. [2], discussed the shrinkage-cracking behaviour of a plain wall with edge restraints built with high-strength mortar. The results showed that the cracking was observed as the (L/H) ratio was eight or greater, which was explained by the nature of the high-strength mortar used. Kheder, G. et. al. [6] investigated the cracking behavior of base-

*Corresponding author: st.yasmeen.N@ced.nahrainuniv.edu.iq
[a]orcid.org/ 0009-0000-2583-3250, [b]orcid.org/ 0000-0003-4282-7068
DOI: http://dx.doi.org/10.17515/resm2026-1265ic1015rs

restrained reinforced concrete walls resulting from volume changes. The primary and secondary space measurements of the cracks and width observed in certain 61 full-size walls and the 14 wall-Experimental walls reveal that due to the disuneveness in the distribution of crack width throughout the wall height, the percentage of reinforcement can change according to wall height. Elwakeel et al. [7] and Shezad [8] examined the behaviour of edge reinforced walls built with a concrete L/H ratio of 4. Elwakeel et al. [7] explained the presence of a visible crack among one of four walls as the ratio of L/H was raised to 5, whereas Shezad [8] also found two out of four walls to crack.

Guidelines on how to control crack widths by judicious reinforcement design are given by Forth [9], Bamforth [10], and Jedrzejewska et al. [11], and aimed to reach a satisfactory level of performance. These guidelines also outline the plans for reducing the risks, such as the potential planning of the pour sizes, the choice of the right materials and mix designs, and the use of efficient construction sequences. In addition, they promote insulation to reduce thermal gradient, pre-cooling or in-situ cooling of concrete, and the introduction of movement joints. Gilbert [12] introduced a principle of controlling the cracking that occurs in early-age concrete due to cooling and shrinkage. This study also evaluated the level of restraint existing in a range of practical concrete with reinforcements and also defined the necessary reinforcement to reduce early age cracking. Al-Zuhairi [13] analyzed the behaviour of mass concrete structures in the presence of variation of temperature and change in volume as a consequence of drying shrinkage through the use FORTRAN and ANSYS softwares. To determine the maximum crack width and the development of strains and stresses in the fixed-end walls, the findings were found to be consistent with the estimated findings of the procedure to be used in the development, using ACI Committee 207. Do et al. proposed a computation programme[14] in MATLAB to assess both the temperature evolution, stress development, and the probability of early-age cracking in the pier-cross-sections with normal-strength concrete (NC) and high-strength concrete (HSC) in the first 7 days after casting. They discovered that in minimising the risk of structural cracking and streamlining construction periods, special considerations in the design and construction of contemporary concrete materials (e.g. the high-strength and high-performance concrete) are justified. Micallef et al. [15] examined the long-term cracking characteristics of reinforced concrete walls when put under combined end and restraining restraints. The results indicate that, with C660, a good estimate of the long-term crack width could be found, but it is prone to overestimating the distance between the cracks. The studies mentioned above clearly indicate that the majority of research concerning early surface cracks has predominantly concentrated on models utilizing normal-strength mortar based on ordinary Portland cement, frequently without incorporating coarse aggregates. Such an approach limits its ability to accurately depict the behavior of structural concrete in real-world scenarios. Moreover, some of these investigations were conducted under controlled laboratory conditions, which did not adequately account for the actual effects of varying field conditions, such as elevated temperatures and rapid moisture loss. Consequently, this affects the realism of the findings that represent the performance of concrete elements in actual environments.

The objective of the present study is to understand how high-performance concrete affects the thermal and shrinkage behaviour of edge-restrained concrete walls. Moreover, it aims to identify how the L/H ratio can vary, which is a critical parameter in this context. In this regard, there were five scaled-down walls that were cast during the summer months and were exposed to the environmental factors to model the real-world exposure.

2. Experimental Program

2.1. Materials

During the summer, two sets of reinforced concrete walls were cast, utilizing two different compressive strengths: normal-strength concrete with a compressive strength of 33 MPa and high-performance concrete with a compressive strength of 62 MPa. The cement used in this study is a standard Portland type which follows the specifications set out in EN 197[16]. Major physical and chemical properties of this cement are shown in Table 1.

- The high-performance concrete incorporated sand characterized by its natural fineness modulus of 2.96, a specific gravity of 2.63, a Sulfate content was 0.365%, and particles exhibiting a predominantly spherical morphology.
- The concrete mixture incorporated a coarse aggregate with a nominal maximum size of 17mm. This aggregate exhibited a specific gravity not exceeding 2.55, water absorption up to 0.48%, and sulphate content of 0.087%. Particle size distributions for both coarse and fine aggregates are detailed in Tables 2 and 3, respectively.
- A polycarboxylate-based superplasticizer, commercially available as Max B 500, was incorporated into the mixture. This admixture, conforming to ASTM C494 Types A and F, exhibited a specific gravity of 1.06.
- Silica fume is an extremely fine powder with a specific gravity of 2.25. Based on trial mixes, 8.33% by weight of the cement was replaced with silica fume from the brand Sika.
- The reinforcing steel that was used was deformed bars with nominal diameters of 8 mm and 10 mm; detailed specifications are shown in Table 2. The reinforcement ratio in steel was more than standard minimums according to British Standard BS 8007[17], American Concrete Institute ACI 318[18], and European Standard BS EN 1992-1[19].

Concrete mixtures were prepared in a laboratory-grade electrically powered mixer in order to ensure homogeneity of the blend. First, the dry constituents, namely cement, aggregate (fine and coarse) were used, then all constituents remained till a uniform colour is achieved. Subsequently, the water was added, mixed for 3 to 5 minutes to attain the desired workability. In the case of high-performance concrete, silica fume was pre-blended with dry. After this dry-mixing stage half of the total water (pre-mixed with the superplasticizer) was added and mixed for about four minutes. The rest of the water was then added and the mixture was blended for three minutes again before it went into the formwork.

Each set of reinforced concrete walls, along with the control specimens associated with each wall set, was cast in a single batch. The control specimens were six cubes (150 by 150 mm for compressive strength determination), For the experimental program, the following specimens were prepared: three 150 mm x 300 mm cubes for heat of hydration analysis; nine 150 mm x 300 mm cylinders for indirect tensile strength evaluation; six 150 mm x 300 mm cylinders for compressive strength assessment; and three 100 mm x 100 mm x 400 mm prisms for flexural strength (modulus of rupture) determination. The concrete was consolidated within the formwork using an electric vibrator during the casting process.

Table 1. Details the physical, Mechanical, and chemical properties of the cement used in this study [20]

Category	Parameter	Value
Chemical composition	Tricalcium aluminate (C_3A)	6.31%
	Magnesium oxide (MgO)	2.49%
	SO_3	2.29%
	Ignition loss	2.45%
	Insoluble residue	0.73%
Physical properties	Blaine surface area	3154 cm^2/g
	Initial set time	114 min
	Final set time	2 hr 42 min
Mechanical property	Compressive strength at 2 and 28 days	25.7 MPa, 46.5 MPa

Table 2. Details the grading requirements for coarse aggregate [20]

Sieve opening (mm)	Material passing (%)	Standard allowable limits
20	100%	100
14	91%	100–90
10	81%	85–50
5	5%	50–0
2.36	0	–

Table 3. Details the sand grading requirements as defined by Iraqi specifications [20]

Sieve (mm)	Acceptable range	Passing (%)
4.75	90–100%	97.4%
2.36	75–100%	75%
1.18	55–90%	68.6%
0.6	35–59%	40.3%
0.3	8–30%	28.2%
0.15	0–10%	2.1%

2.2. Edge-Restrained Concrete Wall Casting

The edge restraint for the walls was achieved using a rigid steel beam, as demonstrated in Micallef [15]and Mushchil et al. [5]. This method simplifies boundary condition modeling, as steel does not creep or shrink like concrete, which minimizes the time required for shrinkage strain relief at the base. This process can take months for structural restraint, as noted by [1, 3, 4]. The steel used was a W-shaped beam, 165 mm high and 100 mm wide. To enhance base roughness, four 10 mm deformed steel bars were welded to the upper surface. All the models have a constant height (50 cm) and thickness (10 cm) , see Figure 1. Table 4 illustrates the models' details, casting of the walls is presented in Figure 2.

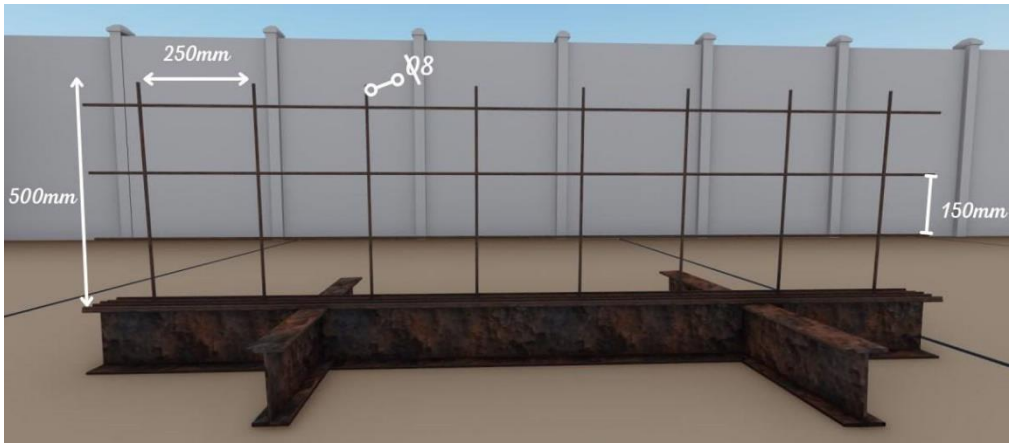

Fig. 1. The wall details

Table 4. The dimensions and reinforcement details of the casted walls

Set num.	L/H	Vertical Reinf.	Horizontal Reinf.	Notation	Concrete Type
Set 1:	5	Ø8@250	Ø8@150	W-NSC-2.5-Ø8	Normal-strength concrete (NSC)
	5	Ø10@250	Ø10@150	W-NSC-2.5-Ø10	
	10	Ø8@250	Ø8@150	W-NSC-5-Ø8	
Set 2:	5	Ø8@250	Ø8@150	W-HPC-2.5-Ø8	High-performance concrete (HPC)
	10			W-HPC-5-Ø8	

2.3. Curing and Exposure

To reduce a potential early-age cracking problem (from rapid moisture loss) the newly formed walls and reference specimens were temporarily covered with plastic sheeting. Subsequent to demoulding, a seven-day wet curing regime was introduced using damp cloths, which were re-moistened periodically to ensure adequate hydration levels. Following this, the specimens were exposed to lab ambient conditions without specific environmental controls. Crack initiation and propagation were monitored over time and thus provided data relevant to the long-term performance of the concrete. A summary of the casting parameters for each of the batches is shown in Table 5 and is further illustrated in Figure 3.

Fig. 2. (a), (b), (c) preparing walls, (d) casting, (e) curing, (f) strain installation., (g) The five hardened walls

Table 5.The casting conditions

The walls	Time of casting	Weather temp.	Concrete temp.	Humidity
NSC-group HPC-group	12 am	33°C	(26-27) °C	At night= 30 At day =20

(a) (b)

Fig. 3. The devices used to record details during casting (a) Humidity and temperature of the weather, (b) Measuring concrete temperature during mixing

3. Deformation, Crack Size, and Hydration Heat Measurements

3.1 Deformation Measurements

After demolding, three 8 cm strain gauges were installed on a polished concrete surface. They were positioned at the centre of the surface at 5 cm, 25 cm, and 40 cm heights from the base for comprehensive strain data collection across different depths in the concrete structure, as shown in Figure 4.

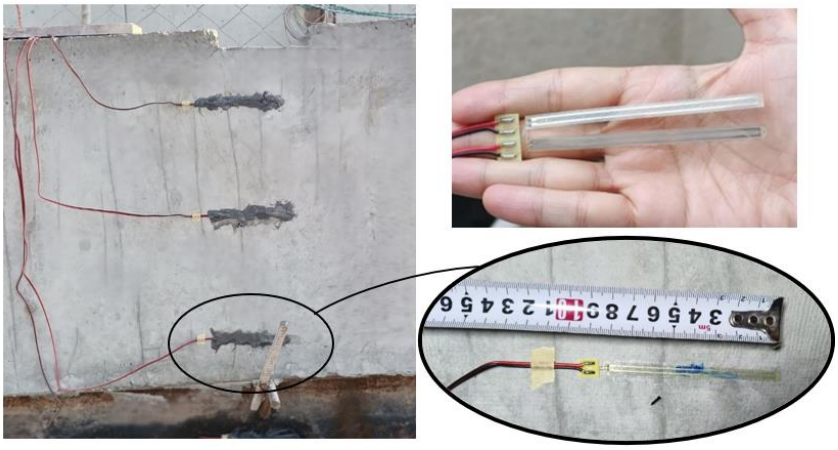

Fig. 4. The 8 cm strain installation

3.2. Crack Width Measurement

A crack meter, which is a portable microscope providing 40X magnification, was used to measure crack widths accurately. It has a 4 mm measuring field for precise observation of crack characteristics (see Figure 5a).

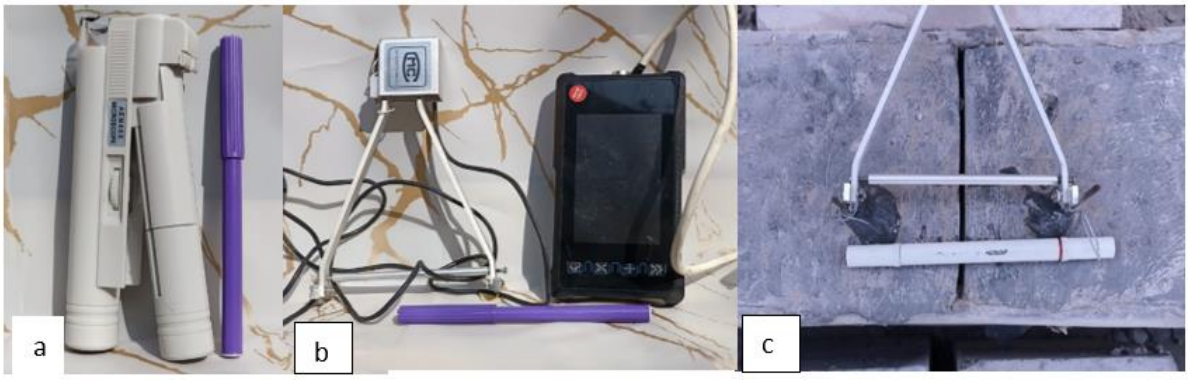

Fig. 5. (a) Crackmeter, (b) and (c) the extensometer installation

An extensometer was also installed at two DEMEC points on the sides, spaced 10 cm apart, to assess changes in free volume in the restrained concrete beam. Frequently, a digital reader with 0.002 mm accuracy connected to the extensometer recorded data until no significant increase in measurements was observed (see Figures 5 b and c).

3.3. The Heat of Hydration Measurement Techniques

It is important to mention that no prior research has examined the heat produced as part of the hydration process along these lines, and the techniques described above have not applied in this context. his study investigates the relationship between the volume and geometry of a structure and the heat generated by cement hydration under realistic conditions. Furthermore, it studies the critical role of ambient temperature and especially its control on heat release and dissipation with time.

A similar method of observing the development of temperature in a concrete member was adopted by Wu [21], in which he used a custom-built data logging system to record the temperature and strain every second. In this study, the same technique is applied to analyse the evolution of the temperature during the hydration in the beam specimens and in the control samples.

- Cube control specimens' technique: To establish a reference for internal heat development, 150 x 150 mm control cubes were cast. A thermistor was embedded at the geometric center of each cube to measure temperature. The cubes were formed using 18mm plywood molds (Figure 6). The data obtained from these control cubes were then compared to the internal temperature measurements recorded in continuous strip beams.
- Edge-restrained wall technique: A thermistor was used to monitor the internal temperature variations within the concrete. It was installed at two points - 150mm and 400mm above the base. The internal temperature at both locations was continuously recorded for 1 week.

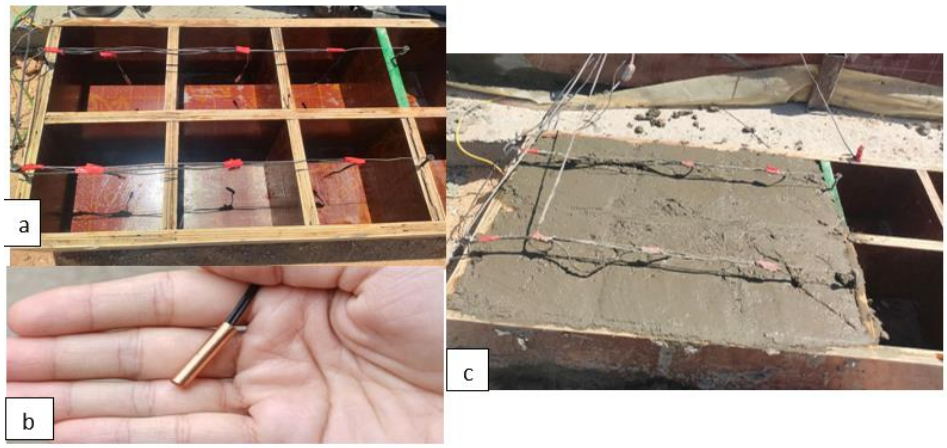

Fig. 6. (a) The thermistor installation, (b) the thermistor, and (c) after casting

4. Tests for Mechanical Performance of Concrete

- Concrete cylinders with dimensions of 150 mm in diameter and 300 mm in height were tested for tensile splitting strength after curing periods of 3, 7, and 28 days. The tests were performed according to the ASTM C496 standard [24]. The testing setup is shown in Figure 8.
- The compressive strength of concrete: The compressive strength test was performed on 150 mm cubes, which were cured for 7 and 28 days in water as per BS EN 12390-3 [16] and above 150 x 300 mm concrete cylinders as per ASTM C39 [23]. The setup of the testing is depicted in Figure 7.
- The modulus of rupture was evaluated using 100 mm x 100 mm x 400 mm concrete prisms cured for 28 days, in accordance with ASTM C78 [25]. This testing protocol was applied to both concrete mixes presented in Table 5.

- Free volume change methods: To assess the variation in the free volume of the concrete, a plain concrete beam was cast with the same I-shaped steel mold as in [26] (see Figure 7). An artificial crack (gap) was inflicted in the mid-span by the introduction of a 4 mm plastic diaphragm. The beam was then exposed to the same environmental conditions as the restrained concrete walls. To minimize the friction between the concrete and the mold, two layers of polythene sheets, which were greased, were used. After casting, the beam was covered with a polythene sheet in order to limit the rapid shrinkage of the plastic. This was then cured for 7 days daily and exposed to similar conditions to the wall specimens, and allowed to shrink and move freely.

Table 5. Mix constituents

Mixes constituents (kg/m^3)	M2-HPC	M1-OPC
Fine aggregate(kg/m^3)	1120	950
Coarse aggregate(kg/m^3)	1150	1050
Cement (kg/m^3)	480	350
Slump (mm)	180	70
Silica fume (kg/m^3)	40	----
W/C ratio	0.25	0.44
Superplastisizer (kg)	4.16	----

- The elastic tensile strain capacity of the concrete was identified through the direct method, using the same I-shaped steel mold in [26] (see Figure 7). Plain concrete beams were made and allowed free shrinkage. As soon as the first crack formed, the amount of strain as a result of the elastic recovery of the restrained concrete was measured. The value of the crack width was measured with a microscope, and then the width of the crack was divided by the total beam length, and this value was considered as the elastic tensile strain capacity of the concrete material. All of the tests described were performed on the two mixes presented in Table 5.

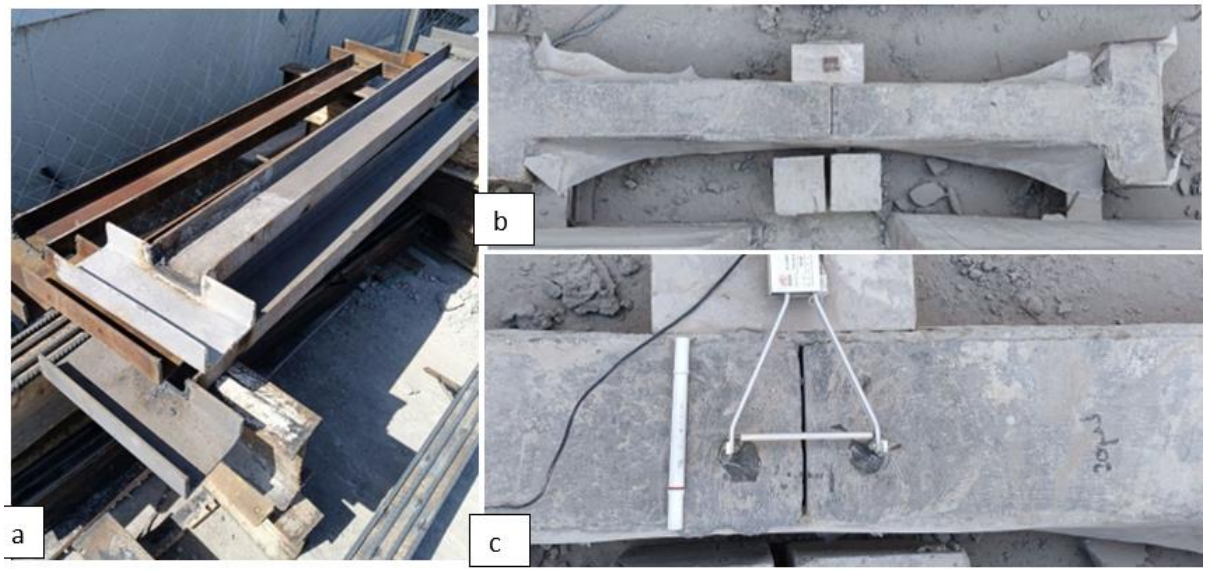

Fig. 7. (a) Mold used for free volume change and elastic tensile capacity, (b) and (c) free volume change method

5. Results and Discussion

5.1. Mechanical Performance of the Concrete Mixes

Table 6 shows the mechanical properties of the concrete for the control specimens of mix M1-NSC and M2-HPC. Each value reported is the average of the values obtained from three individual samples for each mix. The failure patterns on the specimens tested are shown in Figure 8.

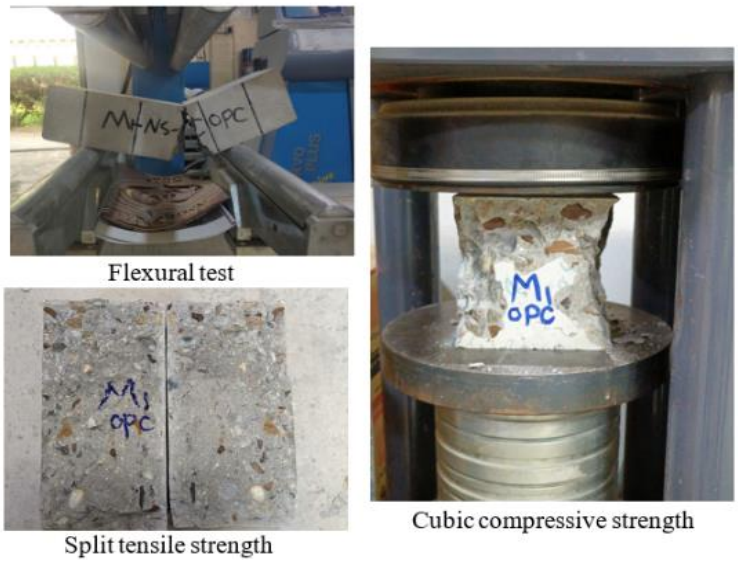

Fig. 8. Control specimens' failure modes

Table 6 shows that the 28-day compressive strength of the cylinder specimens is nearly equal to 0.77 of that of the cubes for normal-strength concrete and 0.78 of that of high-performance concrete. These ratios are very close to those recommended in BS 1881 [27], which recommends cylinder strengths of about 0.8 times corresponding cube strengths. The results also show that the tensile strength for high-performance concrete is stronger than twice that of traditional concrete, indicating a higher level of resistance to cracking - especially during the early life of concrete maturation. In this critical period, the tensile strength is important for reducing the impact of temperature fluctuations and shrinkage that are caused by the proliferation of cement hydration and fluctuations in ambient temperature and moisture. Furthermore, the other mechanical parameters of the concrete mixes show an outstanding uniformity, without recognisable inconsistencies or variation. Together with the results of the compressive strength testing, this consistency shows the reliability and stable working of the materials used.

Table 6. The mechanical properties

Mixes notation	Split tensile strength (MPa)			Flexural strength (MPa)	Cubic compressive strength (MPa)		Cylindrical compressive strength (MPa)	
	3-days	7-days	28-days	28- days	7-days	28-days	7-days	28-days
M1-NSC	1.63	2.2	2.72	2.4	22.07	33.1	13.65	25.6
M2-HPC	2.88	4.12	5.34	6.82	42.6	63.5	40.1	49.6

5.2. Internal Temperature Variation

Analysis of Figures 9 and 10 shows that the temperature variations during the seven days can be divided into two phases. Each phase has specific characteristics that describe what they are doing with the concrete walls and the climatic conditions during the week.

5.2.1 Early Temperature Fluctuations in Concrete Walls Before the Removal of Formwork (Initial Two Days)

All the walls demonstrated comparable thermal behavior during the first two days following casting, irrespective of the type of concrete or wall length. Internal temperatures rose after casting due to the heat generated by hydration, resulting in significant disparities between the internal wall temperatures and the ambient air. Temperatures as shown in Figures 9b, d, f, and Figures 9b, d. This effect was particularly pronounced between the upper and lower parts of the wall. The

upper area, nearer to the surface and directly exposed to sunlight, registered higher temperatures at an accelerated rate than the lower area, which remained cooler. The upper part was cooling down as temperatures declined in the night. However, it did not attain the reading of the surrounding air temperature. This can be explained by the insulating property of the wooden casing of the wall. Therefore, the upper and lower parts of the walls also remained warmer compared to the external temperature until the end of the day, with differences being approximately 5 degrees Celsius for 5-meter-long walls and less than 3 degrees Celsius for the 2.5-meter-long walls. Additionally, the progressive decrease in temperature, principally at the base of the wall, was associated with the effective insulation of the wooden mold that became a barrier to the cooling rate. Such an outcome coincides with the findings of the earlier studies [9, 10, 28], which support the hypothesis that a postponed removal of mold plays a positive role in gradual heat loss and corresponding reduction of the probability of early cracking in concrete.

5.2.2 Temperature Fluctuations in Concrete After the Removal of Formwork

Following the removal of the molds, there was consistent thermal performance within the top and bottom parts of the walls, which was observed two days later. The temperatures at such locations were higher than the ambient air temperature during the day due to their entire exposure to the air from all directions, which permitted the effective absorption of thermal energy during the night as the temperatures steadily declined, hence conforming to the ambient cold temperature. This fall is a thermal loss due to interactions with the external environment, as shown in figures 9a, c, d and figures 10a, c. These patterns illustrate the way the exposed concrete reacts to the conditions provided by the environment, particularly after the removal of the molds, as it becomes more sensitive to the temperature changes in the environment. During the following three days, there was a stabilizing of temperatures, which showed a clear and yet synchronized variation to a daily fluctuation in ambient temperature. This transition means that the concrete has also reached a step where it has a more stable behaviour in terms of thermal contact, lower rate of change and also in terms of its compatibility with its surroundings.

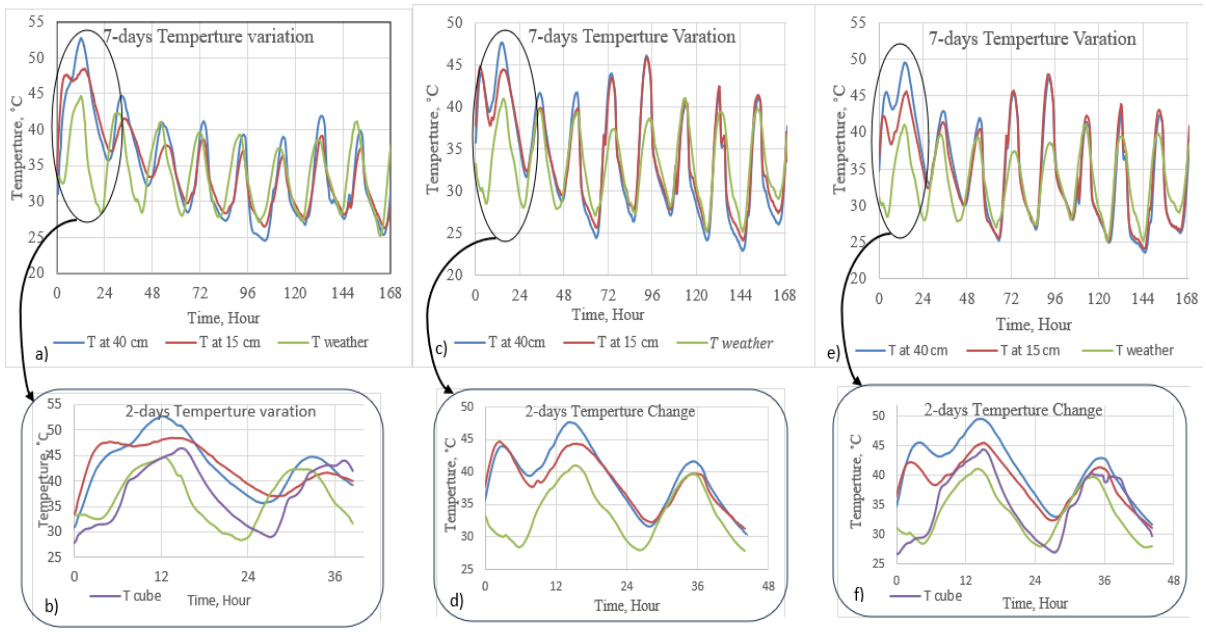

Fig. 9. Inner temperature versus time for the walls: a) W-NSC-2.5-Ø8, c) W-NSC-2.5-Ø10, and e) W-NSC-5-Ø8 for seven days, b, d) and f) their cement hydration

These trends are the normal daily fluctuations in temperature readings, where the trends are rising with higher ambient temperatures during the day and falling in the evening as the day cools down. This interaction describes a well-efficient and comprehensive thermal exchange of the concrete and its surroundings. Overall, this observation emphasizes the significance of the thermal behaviour in the first stage of the concrete existence to the whole state of a structure.

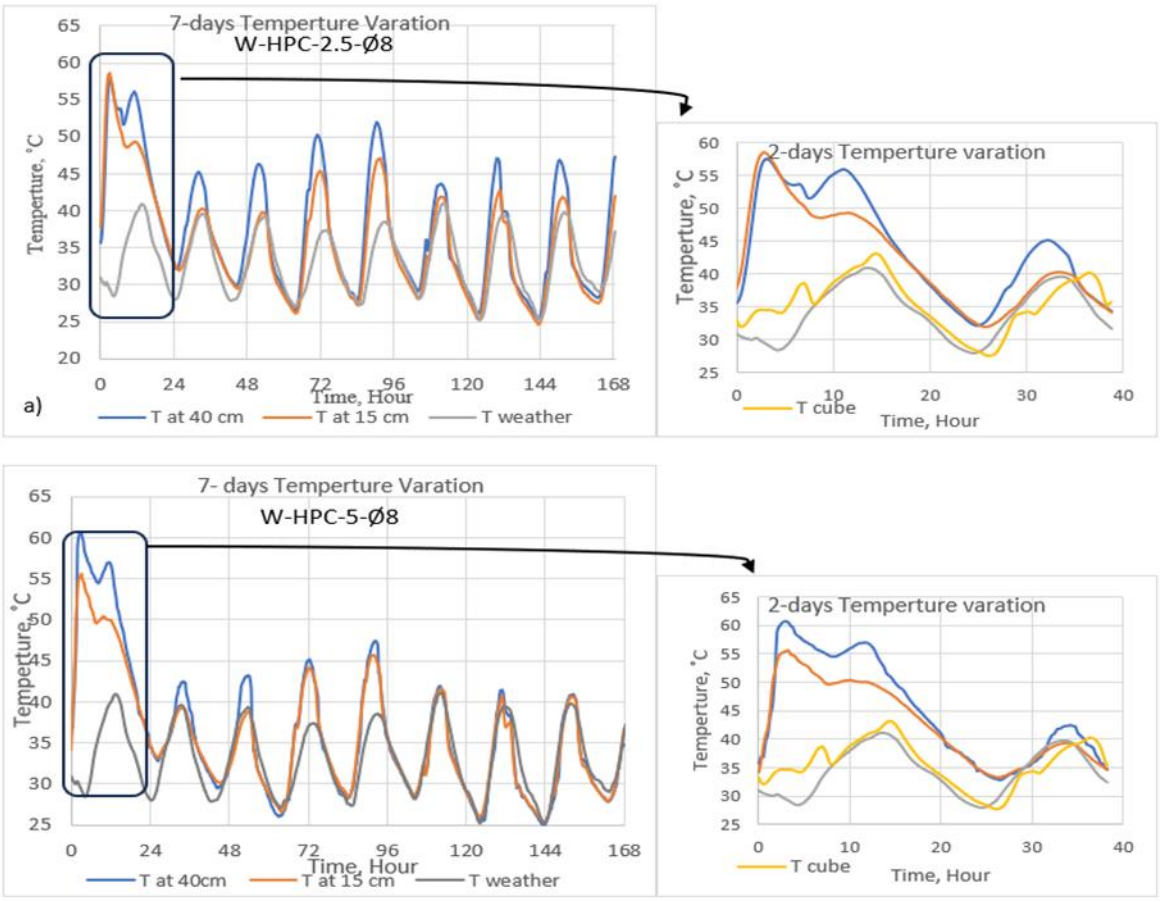

Fig. 10. Inner temperature versus time for the walls: (a) W-HPC-2.5-Ø8 and (b) W-HPC-5-Ø8 for seven days, (c) and (d) during cement

5.2.3 Effect of Concrete Type

The use of high-performance concrete played a crucial role in the determination of temperature development. Different concrete mixes with different cement content and/or additives had an influencing on the peak temperature and cooling rate. Of significance, in the case of the hydration set on HPC as illustrate in figure 10, an increase of higher hydration temperature could be achieved; the higher hydration temperature on the inside of normal strength concrete (NSC) walls reached 45 °C as shown in figure 9, while the higher hydration temperature of the walls of high-performance concrete (HPC) made an impressive mark at 59 °C. This significant variation in temperature influences the properties in the early ages, like the development of strength and cracking risk. These findings show the importance of understanding thermal behavior in order to optimise the mix designs and mitigate the risk of early-age cracking of reinforced concrete structures.

5.2.4 Effect of Length/Height Ratio

The differences between walls and their control cubes in terms of inner temperature result in hydration display drastic variations that are affected by the use of volume and geometry. Normally, the walls contained a slower rate of cooling as compared to the cubes, as seen in Figures 9 and 10. The slower rate can be explained by the large volume to be able to hold heat for a longer time. As this hydration stage went on, the impact of the wall length within the temperature distribution became more apparent, as shown in Figure 8b,f, and in Figure 10b,d. The 5-meter walls showed a lot of difference between the bottom and the top with respect to temperature. Precisely, the temperature of hydration developed on the top of such walls was found to be much higher (8.2% for standard strength concrete and 9.1% for high-performance concrete) temperature at the bottom. On the other hand, the walls with a height of 2.5 meters showed a more homogeneous increase in temperature. Both the top and the bottom point-wise of these shorter walls, however, showed similar rates and values, which provided steadier thermal behavior throughout the

structure. Eventually, the data collected by the recording system indicated a strong correlation between the L/H ratio and peak hydration temperature, in this case, shown especially at the bottom of the walls. Subsequent rises in the inner temperature cause a large difference in temperature between the inner ambient temperature level inside the wall, which is confined within the wall. This difference in temperatures led to the development of thermal cracking that could be seen on the surface of the walls or visible as unobtrusive microcracks within the structure. The second of the mentioned behaviours will be explored further in the next section, focusing on cracking.

5.3. Measurements of Surface Concrete Strain

The strain was measured carefully at three different heights and on every wall, and recorded one week after the walls had fully cured and had reached the required strength. Data collection still went on for more than a month in September, a time when temperature fluctuations were quite extreme, which had dramatic effects on the expansion and contraction cycles of the concrete. The strains visible in the pictures of Figures 11 to 15 are easily detected with positive values indicating expansion and negative values indicating shrinkage. Detailed analysis of these numbers revealed an overall trend flow within all five walls, regardless of the materials they were made from. Normal Strength Concrete (NSC) Excel HPC. This trend can be divided into several phases, each of which emphasises the dynamics of concrete behaviour under conditions of varying environmental conditions:

5.3.1 Phase 1: Concrete Strain Behavior During the First 10 Days After Curing

During this phase, there was a predictable strain response pattern to all vertical locations of the walls (top, middle, bottom) for the differences in the concrete mix. Strain values showed significant changes due to changes in the temperature. An Increase in daytime temperature is observed to produce considerable shrinkage in the concrete during daytime, and low temperature at night produces little expansion. This behavior is in line with well-recorded concrete thermal properties, which imply its sensitivity to temperature changes. Additionally, the strain data gave small differences between the measurements at the three vertical levels, showing uniform moisture losses in the walls and good curing. Notably, the accumulated strain through shrinkage was much higher as compared to that of expansion, which signified a strong tendency to shrinkage. Tables 7 and 8 conclusively summarize the average shrinkage and expansion strain values obtained for the five walls in this phase.

5.3.2 Phase 2: Strain Behavior from Day 10 to Day 20

From the onset of this phase, the behavior of the strain mainly tended to shrinkage, and the expansion strain noted at the beginning of the phase decreased significantly. Three significant observations were made:

- Volatilities in values of the strains among the three vertical positions were amplified as a result of the difference in the degree of moisture loss that resulted from temperature changes. These differences emphasized the individual effects of environmental conditions on every position.
- Walls of larger lengths of 5 m only experienced shrinkage strain, while the short walls of 2.5 m recorded a small amount of expansion strain. This observation marks the role of the length-to-height (L/H) ratio, whereby longer structures are more prone to large shrinkage. This complies with the researchers' results [1- 5,7].
- Drying shrinkage became the biggest control of strain characteristics, worsened by temperature fluctuations during the day. These cycles of environmental impacts amplified the effects of shrinkage, focusing on the material behavior and the structural integrity that was induced with time.

5.3.3 Phase 3: Strain Behavior after Day 20

Following 20 days, all five walls exhibited elevated values in strains compared to the previously phases with little substantial reduction in the shrinkage strain noted during nighttime, which adheres to Wu [21]. This means that shrinkage strains continued to add to one another, causing

restrained tensile stresses in the concrete. The possibility of cracks developing if these stresses exceed the tensile strength of the material.

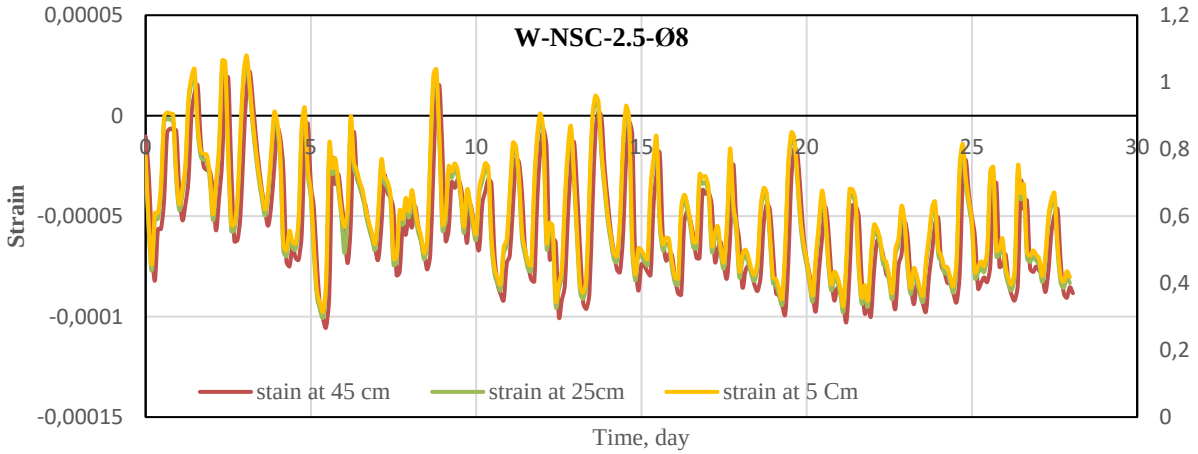

Fig. 11. Measured surface concrete strain versus time for W-NSC-2.5-Ø8

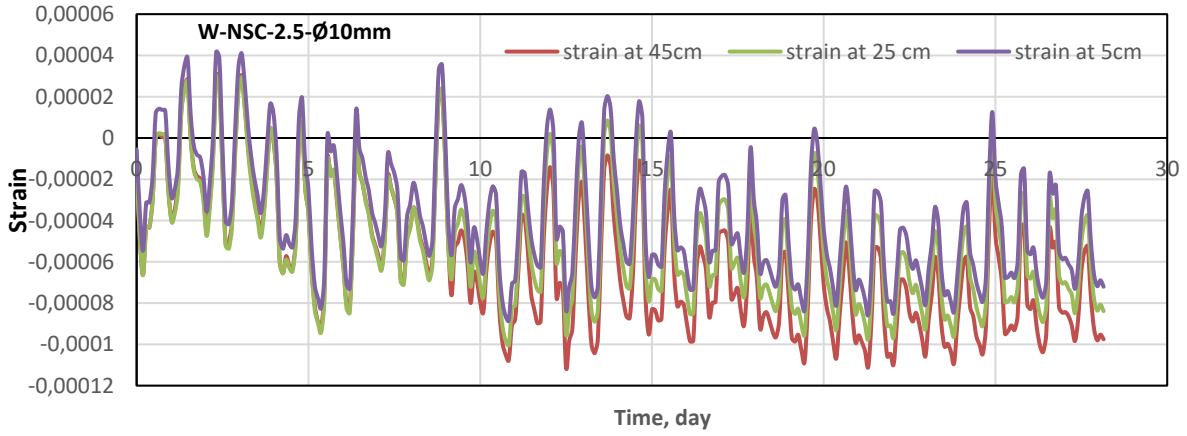

Fig. 12. Measured surface concrete strain versus time for W-NSC-2.5-Ø10

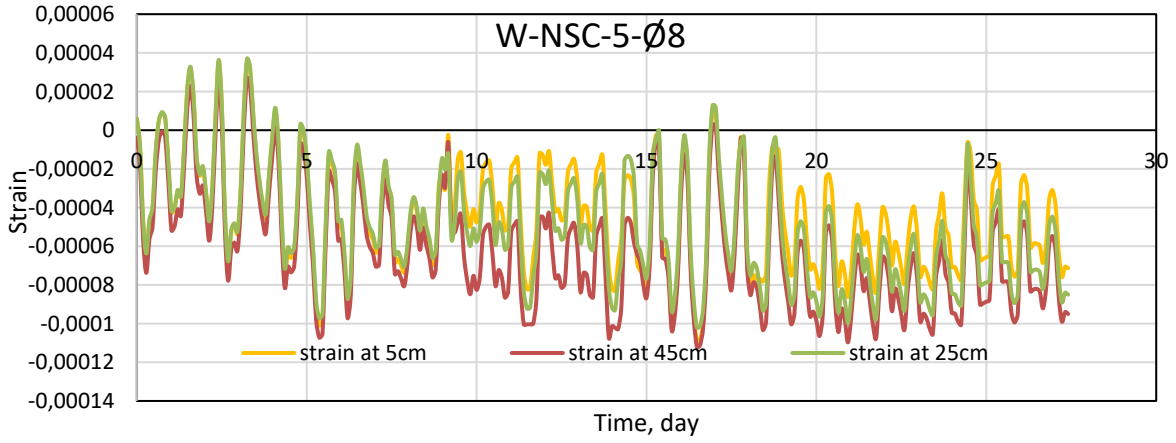

Fig. 13. Measured surface concrete strain versus time for W-NSC-5-Ø8

5.4 Effect of Steel Reinforcement

The effects of increasing the size of reinforcement bars from 8 mm to 10 mm were clearly observed in the strain distribution across different levels of the wall, as shown in Figure 12. Compared to the reference wall in Figure 11, the wall reinforced with the larger 10 mm bars exhibited subtle yet significant differences in strain levels from the very first day of observation. Such differences

became much more noticeable after the first round of testing and kept on growing throughout the entire evaluation period. In addition, the wall with the 10 mm reinforcement showed much more expansion strain level in comparison with the reference wall; thus, the reinforcement bar size had a strong effect on the wall's response to environmental conditions. Notwithstanding this extraordinary increase in the expansion strain, the overall shrinkage strain remained the dominating factor, thus confirming that the wall generally shrank with time. Such findings point out the significant role played by the reinforcement bar sizes on the strain distribution as well as the long-term nature of deformation of the wall. Additionally, they show the use of bigger bars of steel as per the allowable specifications, which can be important in removing the early age cracking that typically emanates due to the temperature and moisture fluctuations in the material.

5.5 Effect of Length/Height Ratio

Strain distribution and the deformation behavior of concrete walls are greatly influenced by changing the L/H ratio. Studying results presented in Figures 11, 13, 14, and 15 show that with an increase in L/H ratio, the concrete strain tends to shift towards shrinkage strain, especially after the first ten days. Additionally, strain increases significantly at this first stage of the analysis, and for longer walls (irrespective of concrete type), peak shrinkage strain values are higher than the reference values. This variation highlights the great effect that the length-to-height (L/H) ratio has on the behavior of walls. When increasing the length of the wall, the area of the wall that will be exposed to varying conditions of the air is considerably increased. This increased exposure not only increases the fluctuations in temperature to which the wall is exposed, but also increases the level of movement of moisture in the concrete. The interaction of these factors can have a significant effect on the structural strength and life of the walls over time.

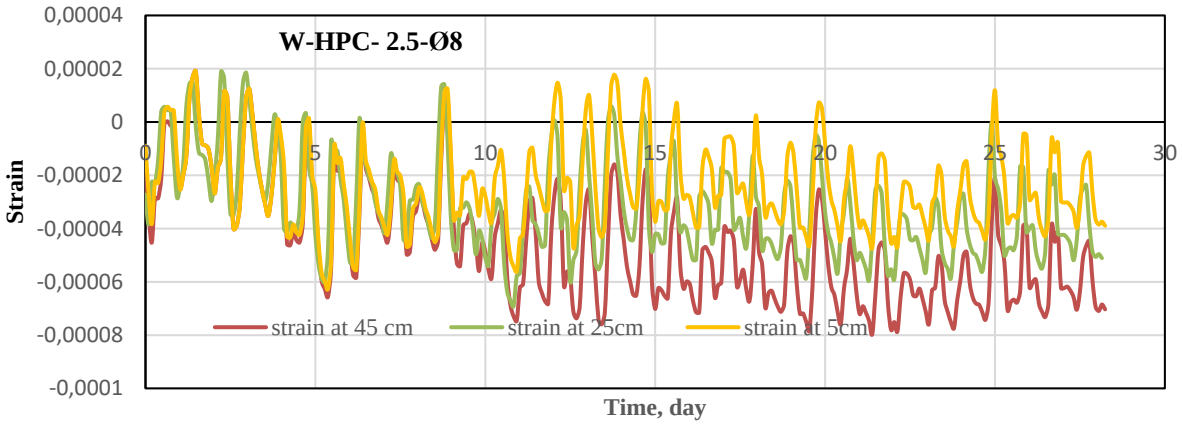

Fig. 14. Measured surface concrete strain versus time for W-HPC-2.5-Ø8

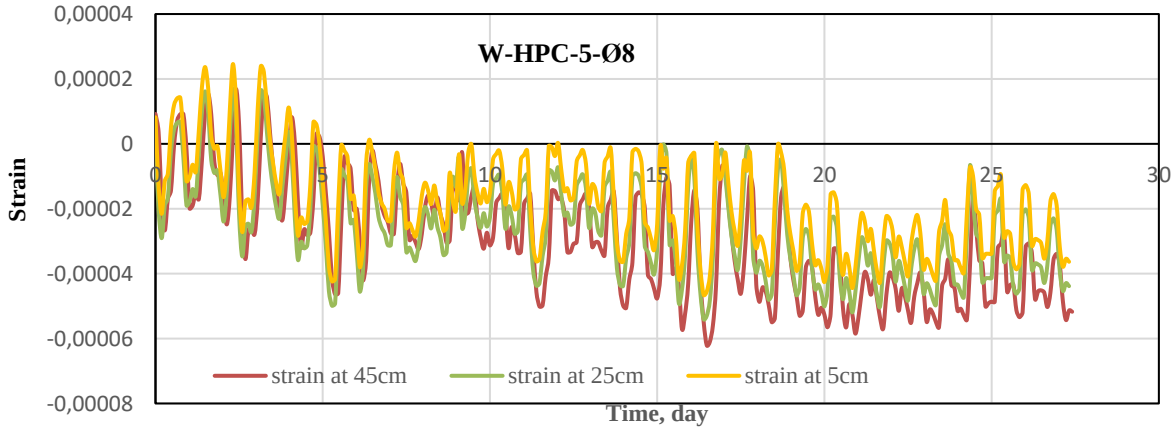

Fig. 15. Measured surface concrete strain versus time for W-HPC-5-Ø8

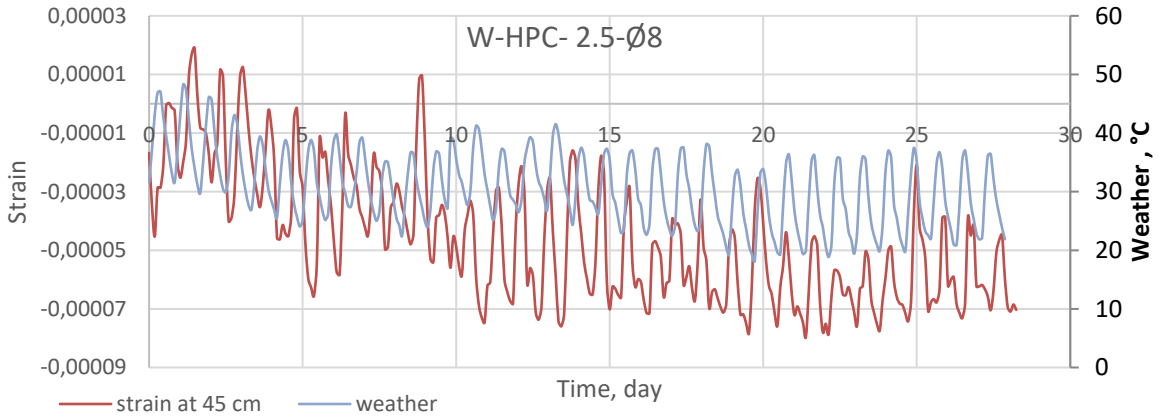

Fig. 16. Concrete strain versus time at 45m from base with ambient temperature for W-HPC-2.5-Ø8

Table 7. Phases of strain development: behaviour, avg max. shrinkage and expansion strain for the NSC group

Phase number	Wall notation	Observed behavior	Avg daily temperature	Avg. shrinkage strain ($*10^{-6}\mu m$)			Avg night temperature	Avg. expansion strain ($*10^{-6}\mu m$)		
				Top	Mid.	Bottom		Top	Mid.	Bottom
Phase 1	W-NSC-2.5-Ø8	Exhibiting perfect fluctuations in response to temperature variations	44	63.83	59	55.8	28	18.7	23.6	14.4
	W-NSC-2.5-Ø10			52.2	53.5	42.2		16.82	16.83	28.8
	W-NSC-5-Ø8			65.83	55.9	57.83		19.4	21.2	34.2
Phase 2	W-NSC-2.5-Ø8	Progressive increase in shrinkage	38	83.2	78.1	74.4	24	8.5	30.1	9.8
	W-NSC-2.5-Ø10	Shrinkage increased, and after the ninth day, the difference between the three levels became noticeable.		89.4	91	69		13.1	7.82	16.1
	W-NSC-5-Ø8			92.5	78.3	74.7		1.76	11.8	10.3
Phase 3	W-NSC-2.5-Ø8	Mainly shrinkage	37	85	89.3	86.3	20	-	-	-
	W-NSC-2.5-Ø10	Mostly shrinkage		103.1	90.4	79		-	0.08	12.6
	W-NSC-5-Ø8	Mainly shrinkage		101	90.78	77.5		-	-	-

Table 8. Phases of strain development: behavior, average max. shrinkage and expansion strain for the HPC group.

Phase number	Wall notation	Observed behaviour	Avg day temperature (ºC)	Avg shrinkage strain ($*10^{-6}\mu m$)			Avg night temperature (ºC)	Avg expansion strain ($*10^{-6}\mu m$)		
				Top	Mid.	Bottom		Top	Mid.	Bottom
Phase 1	W-HPC-2.5-Ø8	Exhibiting perfect fluctuations in response to temperature variations	44	36.2	33.83	34.7	28	14.3	10.4	9.74
	W-HPC-5-Ø8			26.8	27.7	20		11.2	11.9	17
Phase 2	W-HPC-2.5-Ø8	Shrinkage strain increases progressively, and after the ninth day, the difference between the three levels became noticeable.	38	64.2	51.2	42.4	24	9.6	6.22	10.94
	W-HPC-5-Ø8			43	39	32.3		-	-	1.22
Phase 3	W-HPC-2.5-Ø8	Almost shrinkage	37	74.7	55.4	43.1	20	-	-	1.19
	W-HPC-5-Ø8	Mainly shrinkage		54.5	47	40		-	-	-

5.6 Effect of Using High-Performance Concrete

The use of high-performance concrete (HPC) in the wall structures showed similar behavior to that of the regular normal strength concrete walls. However, as can be seen in Figures 14, 15, there were considerable variations in strain data obtained for three different measuring levels. The HPC walls showed lower peaks of stress shrinkage strain as compared to their normal-strength counterparts in Figure 11, which indicated a more stable performance under stress. Especially interesting was the behavior for the W-HPC-2.5-Ø8 wall, which had higher values of expansion strain at the lower level of the measurement, closer to the foundation level, within the period of testing. This peculiar behavior can be explained by the presence of the silica fume in the HPC mix that reacts with the product of the hydration of cement, which is the calcium silicate hydrate or C-S-H. This is true not only in the production of additional pore-filling but also improvement of densification of the concrete structure, where the resistance to shrinkage is greatly decreased. Such a conclusion is in perfect agreement with Neville's [29]: Even with these benefits, it was pointed out that, mostly, the strain accumulation values were negative, meaning there was a tendency by the wall to get smaller over time. On top of that, the disparities in measurements of strains on different levels indicated that the concrete reaction was correlated to a large extent with the conditions of the environment. The natural variations of the temperature and the humidity had a considerable influence on this first type of development of the concrete: the sensitivity of the material to the environment. In summary, the results obtained from this study identify the interplay of various aspects of the attributes of HPC and external factors on the performance of concrete structures.

5.7 Cracking of Edge-Restrained Walls

Strain measurements indicate that the behavior of normal strength concrete (NSC) and high performance concrete (HPC) possesses different properties under usual temperature fluctuations, and especially on the shrinkage issue. Nonetheless, no tangible cracks were noticed in all five walls during the testing time. The fact that there have been no signs of cracking, although there was measurable strain as shown in Figures 11 to 15, can be mostly attributed to the qualities of the concrete mix. The addition of coarse aggregate in the mixture caused micro-cracks to be produced at the interface between the mortar and the coarse aggregate particles. These fine micro-cracks formed around the gravel particles as a result of volume change in the concrete, which was caused

by hydration, curing, and temperature variations. These results are similar to those reported earlier [30, 31], implying that most cracks are at the interface between mortar and coarse aggregates rather than in the mortar itself. In addition, Thomas [31] has distinguished three types of cracks:

- Horizontal and vertical cracks, found nearest to the minimum distance between gravel particles.
- Diagonal cracks, which appear at the maximum separation between gravel particles.
- Cracks at the bond. The first two types of cracks are associated with maximum tension within the paste, while the third type arises from weak bond strength between the sandstone and the paste during the early stages of the concrete setting.

Simultaneously, the findings of this research offer conflicting results when contrasted with another study. For example, Kheder [1] reported that the wall with the length-to-height ratio of 4 developed secondary cracks, and walls with a higher L/H ratio showed both primary and secondary cracks. In contrast, Shehzad [8] observed that with an L/H ratio of 4 two out of four walls were cracked. More recently, Elwakeel et al. [7] investigated three walls of the same aspect ratio with increasing L/H ratio of a fourth wall to 5. The latter wall was subject to cracking, unlike the other three; even though the concrete mix in it was similar to that of one of the other. Additionally, Al-Tameemi [2] showed that edge-restrained walls with the L/H-ratio of 8, which were constructed with a high-performance mortar, suffered from both primary and secondary crack occurrences. From the comparison of the results obtained in this study and the previous research where various length/height (L/H) ratios in walls made of concrete were discussed, it can be concluded that the ratio of length and height affects the crack behavior in the wall. However, it is not the only factor in the game. The inconsistency between studies in findings implies that multiple factors influence this behavior. These include environmental conditions such as temperature and humidity, the type of concrete and the mechanical properties of the concrete, and implementational details such as the type of restraint used, the processing technique, and the timing and technique for formwork removal. Table 8 shows a systematic comparison of the results from this study by comparison with several previous studies. These studies examined concrete walls having similar or different length-to-height ratios taking into account variations in concrete type and environmental conditions.

Table 8. previous researchers' results using concrete for casting the walls

The study	L/H	Using aggregate	Concrete type	Results
Kheder [1]	≥4	Used	NSC	Cracked
Shehzad [8]	4	Used	NSC	2 cracked
Elwakeel et al. [7]	4, 5	Used	NSC	The wall with a ratio of 5 only cracked
Al-Tameemi, et al. [2]	8	Not used	HPC	cracked

6. Conclusion

The results showed that the use of coarse aggregate in the concrete mix clearly contributed to reducing early surface cracks, as the generated microcracks help release part of the internal tensile stresses and prevent their development into visible surface cracks. The study also indicated that the likelihood of early cracking is related to the interaction between the initial thermal rise and the degree of restraint; despite the significant variation between daytime and nighttime temperatures, the internal thermal rise remained within levels that do not generate sufficient tensile stresses to cause visible surface cracks during the first few days. As well as, increasing L/H ratios increases shrinkage strains; the peak shrinkage strain increases with longer walls up to 9.1% compared to shorter walls in the case of HPC, indicating a geometric effect on behaviour at an early age. These results highlight the importance of material composition, structural geometry, and environment in creating long-lasting concrete infrastructure, especially in alleviating early-age distress. Further

researches need to be conducted on full-scale models using concrete mix, to identify the most influential factor among these in preventing the occurrence of cracks.

References

[1] Kheder GF. Control of shrinkage cracking in reinforced concrete walls [MSc thesis]. Baghdad: University of Baghdad; 1986.

[2] Al-Tameemi AA, Attiyah AN, Mohammed TJ. Cracking behavior of base-restrained high-strength plain concrete walls due to shrinkage. International Journal of Scientific Engineering and Research. 2018.: 8(1):1-10. https://doi.org/10.21275/18012001

[3] Al Attar TS. Minimum steel reinforcement for control of cracking due to shrinkage and temperature changes in reinforced concrete tension members [MSc thesis]. Baghdad: College of Engineering, Baghdad University; 1988.

[4] Al Mashhadi SA. Control of secondary shrinkage cracking in reinforced concrete walls [MSc thesis]. Baghdad: College of Engineering, Baghdad University; 1989.

[5] Al-Mashhadi MS, Habeeb GM, Mushchil AK. Control of shrinkage cracking in end-restrained reinforced concrete walls. Int J Archit (IJA). 2019;5(2):41-62.

[6] Kheder GF, Al-Rawi RS, Al-Dhahi JK. A study of the behaviour of volume change cracking in base-restrained concrete walls. Mater Struct. 1994;27:383-92. https://doi.org/10.1007/BF02473441

[7] Elwakeel A, Shehzad M, El Khoury K, Vollum R, Forth J, Izzuddin B, et al. Assessment of cracking performance in edge restrained RC walls. Struct Concr. 2022 Jun;23(3):1333-52. https://doi.org/10.1002/suco.202100688

[8] Shehzad MK. Influence of vertical steel reinforcement on the behaviour of edge restrained reinforced concrete walls [PhD dissertation]. Leeds: University of Leeds; 2008.

[9] Forth JP, Martin A, Anchor RD. Design of liquid retaining concrete structures. [City of publication]: Whittles Publishing; 2014.

[10] Bamforth PB. Control of cracking caused by restrained deformation in concrete. [City of publication]: CIRIA; 2018.

[11] Jędrzejewska A, Zych M, Kanavaris F, Chen F, Ito S, Torrenti JM, et al. Standardized models for cracking due to restraint of imposed strains-the state of the art. Struct Concr. 2023 Aug;24(4):5388-405. https://doi.org/10.1002/suco.202200301

[12] Gilbert RI. Cracking caused by early-age deformation of concrete-prediction and control. Procedia Eng. 2017 Jan 1;172:13-22. https://doi.org/10.1016/j.proeng.2017.02.012

[13] Al-Zuhairi AHA. Control of volume change cracking in plain and reinforced massive concrete with different base restraints [PhD thesis]. Baghdad: College of Engineering, Baghdad University; 2005.

[14] Do TA, Hoang TT, Bui-Tien T, Hoang HV, Do TD, Nguyen PA. Evaluation of heat of hydration, temperature evolution, and thermal cracking risk in high-strength concrete at early ages. Case Stud Therm Eng. 2020;21:100658. https://doi.org/10.1016/j.csite.2020.100658

[15] Micallef M, Vollum RL, Izzuddin BA. Cracking in walls with combined base and end restraints. Mag Concr Res. 2017 Nov;69(22):1170-88. https://doi.org/10.1680/jmacr.17.00026

[16] European Committee for Standardization; British Standards Institution. EN 197-1: Cement. Part 1, Composition, specifications, and conformity criteria for common cements. London: BSI; 2012.

[17] British Standards Institution. BS 8007: Design of concrete structures for retaining aqueous liquid. London: BSI; 1987.

[18] American Concrete Institute. ACI 318M-19: Building code requirements for structural concrete. Farmington Hills (MI): ACI; 2019.

[19] British Standards Institution. BS EN 1992-1: Eurocode 2: Design of concrete structures - Part 1: General requirements. London: BSI; 2004.

[20] Central Agency for Standardization and Quality Control. Iraqi Specification IQS No. 45: Aggregate from natural sources for concrete and construction. Baghdad: COSQC; 1984.

[21] Wu CH, Lin YF, Lin SK, Huang CH. Temperature development and cracking characteristics of high strength concrete slab at early age. Struct Eng Mech. 2020 Jun 25;74(6):747-56.

[22] British Standards Institution. BS EN 12390: Testing hardened concrete, method of determination of compressive strength of concrete cubes. London: BSI; 2000.

[23] ASTM International. ASTM C39/C39M-15a: Standard test method for compressive strength of cylindrical concrete specimens. West Conshohocken (PA): ASTM; 2015.

[24] ASTM International. ASTM C496: Standard test method for splitting tensile strength of cylindrical concrete specimens. West Conshohocken (PA): ASTM; 2004.

[25] ASTM International. ASTM C78/C78M-16: Standard test method for flexural strength of concrete (using simple beam with third-point loading). West Conshohocken (PA): ASTM; 2016.

[26] Al-Rawi RS. Determination of tensile strain capacity and related properties of concrete subjected to restrained shrinkage. In: Proceedings of ACI Symposium; 1985 Aug; Singapore. p. 18.
[27] British Standards Institution. BS 1881-120: Testing concrete. Method for the determination of the compressive strength of concrete cores. London: BSI; 1983.
[28] Anchor RD. Design of liquid retaining concrete structures. 2nd ed. [City of publication]: [Publisher Name]; 1992.
[29] Neville A. Neville on concrete. Farmington Hills (MI): American Concrete Institute; 2003 Jan 1.
[30] Meyers BL, Winter G. Relationship between time-dependent deformation and microcracking of plain concrete. J Proc. 1969 Jan 1;66(1):60-8. https://doi.org/10.14359/7342
[31] Thomas TC. Mathematical analysis of shrinkage stresses in a model of hardened concrete. J Proc. 1963 Mar 1;60(3):371-90. https://doi.org/10.14359/7860